Agricultural and Forest Meteorology 154–155 (2012) 203–213

Contents lists available at SciVerse ScienceDirect

Agricultural and Forest Meteorology

journal homepage: www.elsevier.com/locate/agrformet

Are rain-induced ecosystem respiration pulses enhanced by legacies of antecedent photodegradation in semi-arid environments?

Siyan Ma[a,*], Dennis D. Baldocchi[a], Jaclyn A. Hatala[a], Matteo Detto[b], Jorge Curiel Yuste[c]

[a] Ecosystem Science Division, Department of Environmental Science, Policy and Management, University of California at Berkeley, 130 Mulford Hall # 3114, Berkeley, CA 94720, USA
[b] Smithsonian Tropical Research Institute, MRC0580-06, Unit 9100 Box 0948, DPO AA 34002-9998, USA
[c] CREAF (Centre de Recerca Ecológica i Aplicacions Forestals), Unitat d'Ecofisiologia i Canvi Global CREAF-CEAB-CSIC, Edifici C, Universitat Autònoma de Barcelona 08193 BELLATERRA (Barcelona), Spain

ARTICLE INFO

Article history:
Received 7 March 2011
Accepted 22 November 2011

Keywords:
Soil
Respiration
Ecosystem
Labile carbon pool
Mediterranean climate
Drought
Annual grassland
Peatland pasture

ABSTRACT

Ecosystem respiration (R_{eco}) is highly variable in semiarid ecosystems. After a period of drought, R_{eco} can jump to a high value in response to rain events, and afterward it decays exponentially with time. To better understand the timing, size, and duration of rain-induced respiration pulses, we examined 57 rain events from over 23 site-years of eddy covariance measurements at an open annual grassland, a woodland understory, and a peatland pasture in California, USA. To explain these findings, we conducted a factorial litter-watering experiment on grass and soil plots exposure to varying amounts of sunlight and water. To interpret and compare the population of rain-induced respiration pulses, we fitted the data with a two pool, 4-parameter exponential decay model.

At the field scale, the total amounts of CO_2 emission emanating from a single and sustained respiration pulse (mean ± standard deviation) were 44.4 ± 38.0, 24.2 ± 17.8, and 94.6 ± 45.8 gC m^{-2} at the open grassland, the woodland understory, and the peatland pasture, respectively. The large variations in precipitation of these respiration-triggering rain events were associated with 73–84% of variation in the total amount of CO_2 emission.

Litter that experienced antecedent photodegradation tended to enhance respiration pulses. Biotic and abiotic processes involved in the dynamic of respiration pulses were pulse-specific, and we summarized them into two pulse scenarios. This study illustrates an emerging connection of ecosystem processes, and these findings may help to improve models on the dynamics of ecosystem CO_2 cycling.

Published by Elsevier B.V.

1. Introduction

Ecosystems in semi-arid climates (e.g., Mediterranean type) experience distinct phenological periods when soil moisture is abundant, declining, or lacking. These distinct hydrological regimes are important because they impose different biophysical controls on ecosystem respiration. During the wet winter, respiration is controlled mainly by temperature, plant and root activity, and the size and digestibility of the organic carbon pool. Between the wet winter and dry summer seasons, the decline in soil water potential restricts the metabolic activity of the plants, roots, and microbes and reduces ecosystem respiration (Baldocchi et al., 2004; Qi and Xu, 2001; Reichstein et al., 2002). When soil moisture hovers below 10% volumetric water content and grasses are dead, ecosystem respiration proceeds at depressed, basal levels (Xu and Baldocchi, 2004). The resumption of rain events following a long dry period is often associated with a marked pulse in respiration, followed by a prolonged exponential decay as the soil dries (Huxman et al., 2004; Jarvis et al., 2007; Lee et al., 2004; Xu et al., 2004). Respiration pulses, induced by rain after a period of drought increase the turnover rate of soil organic matter. In soil science, the rain induced respiration pulse is known as the "Birch Effect" (Birch, 1958; Fierer and Schimel, 2003; Jarvis et al., 2007) and it is a special case of soil respiration priming (Kuzyakov et al., 2000).

Rain-induced respiration pulses are important factors in determining an ecosystem carbon balance. First, rain-induced respiration pulses can exceed respiration rates expected as a result of simple temperature and soil moisture response functions (Qi and Xu, 2001; Reichstein et al., 2002) by an order of magnitude (Jarvis et al., 2007; Xu et al., 2004). Second, rain-induced respiration pulses can be responsible for more than 10% of the carbon lost by an ecosystem over a year (Jarvis et al., 2007; Xu et al., 2004). Despite these implications, the complex and dynamic behavior of rain-induced respiration pulses remain poorly quantified, from a synthesis perspective. Few, if any, ecosystem carbon cycling models possess mathematical algorithms that simulate the complex,

* Corresponding author. Tel.: +1 510 642 2421; fax: +1 510 643 5098.
E-mail address: syma@berkeley.edu (S. Ma).

0168-1923/$ – see front matter. Published by Elsevier B.V.
doi:10.1016/j.agrformet.2011.11.007

temporal dynamic of rain-induced respiration pulses in a realistic and mechanistic fashion (Jarvis et al., 2007; Xu et al., 2004). Therefore, better quantification of the factors that control respiration pulses may lead to the incorporation of pulse-induced carbon cycle losses into carbon cycle models.

Rain-induced respiration pulses are associated with physical, chemical, and biological mechanisms. For example, CO_2 is flushed out immediately when air is pushed out of soil pores by the wetting front. Although in soil pore spaces CO_2 concentrations can be quite high (several thousand parts per million), the effective volume occupied by the air is small. Consequently, this physically mediated efflux is small compared to the magnitude of carbon dioxide that is liberated by the rapid resumption of microbial respiration (Fierer and Schimel, 2002; Inglima et al., 2009; Xu et al., 2004).

The biological forcing of respiration pulses is primarily associated with soil microbial activities (Baldocchi et al., 2006; Fierer and Schimel, 2002; Kuzyakov, 2006; Unger et al., 2010). In principle, a rain event causes a sudden increase in soil water potential which in turn: (1) re-hydrates dormant microbes, (2) breaks down soil micro-aggregates that protect soil organic carbon, and (3) induces microbial cell lysis, a process that releases cytoplasmic solutes. These steps make carbon substrates accessible to surviving soil microbes and thereby stimulate their growth, metabolic activity, and reproduction. Together, these factors promote rapid increases in respiration on short time scales and enable elevated CO_2 effluxes to be sustained for days as the soil dries (Austin and Ballare, 2010; Austin and Vivanco, 2006; Brandt et al., 2009; Moorhead and Callaghan, 1994).

In theory, the size of rain-induced respiration pulses depends on the amount of rain and the size of soil carbon pool (Fierer and Schimel, 2003; Kuzyakov et al., 2000). Given the same amount of rain, soils with carbon pools having short turnover times may support larger respiration pulses than those possessing long lived carbon pools. However, Xu et al. (2004) reported that rain-induced respiration pulses from the open grassland were greater than those from the shade of the oak woodland understory, even though the oak woodland understory contains a soil carbon pool with a shorter turnover time (Curiel Yuste et al., 2007). This exception suggests that additional factors may also be important in determining the size and response curve of respiration pulses. Also, depending on the timing, a small rain event could liberate more CO_2 than a subsequent large rain event (Xu et al., 2004).

Contradictions between theory and practice lead us to consider a broader set of ecosystem processes in predicting the size and dynamics of respiration pulses. New evidence on dry-season photodegradation (Rutledge et al., 2010) implies a possible connection between the size of rain-induced respiration pulses and the legacy of labile carbon produced by photodegradation.

Photodegradation is a photochemical process associated with the breakdown of the molecular structure of litter by direct sunlight (Austin and Vivanco, 2006; Brandt et al., 2009; Henry et al., 2008; Moorhead and Callaghan, 1994; Rutledge et al., 2010). Photodegradation causes direct CO_2 emissions from dry litter during the dry season and it facilitates and breakdown of coarse litter remnants in the field (Henry et al., 2008; Moorhead and Reynolds, 1989). The photo-degraded plant litter could be a labile C source to soil microbes.

We hypothesize that photo-degraded litter could be a labile C source for soil microbes when water leaches through litter. We also hypothesize that more labile carbon will be produced from open grassland sites compared to shaded ones, or in proportion with the duration of sunshine prior to a rain event. This labile carbon will be consumed readily by microbes, and contribute to the rain-induced respiration pulse. Because the size of this photo-degraded labile carbon pool is limited, smaller pulses of soil respiration are expected from sequential rain events, given the same amount of precipitation.

To test these hypotheses, we evaluated a dataset of rain-induced respiration pulses that we collected from a decade-long study of carbon dioxide flux measurements from an annual grassland and the shaded grassland of an oak woodland in California, when the grass was dead. The interpretations of these data were augmented with a set of manipulative watering field experiments on grassland plots exposed to different amounts of sunlight. We also compared these grasslands with a drained and degraded peatland pasture that had highly organic soils and live vegetation. The objectives of this paper are the following: (1) to characterize the timing, size, and duration of rain-induced respiration pulses for different light conditions, (2) to examine biotic and abiotic factors related to the dynamic features of the rain-induced respiration pulses, and (3) to test for the effects of photodegradated litter on the size and dynamics of subsequent rain-induced respiration pulses.

2. Methods

2.1. Study site

Our study sites included an open annual grassland (Vaira Ranch: 38.24°N, 120.57°W, 129 m altitude), the understory grassland of an oak/grass savanna (Tonzi Ranch: 38.43°N, 120.97°W, 177 m altitude), and a drained, degraded peatland pasture (Sherman Island: 38.04°N, 121.75°W) in California. The Vaira and Tonzi ranches are located on lower foothills of the Sierra Nevada, near Ione, CA, and are approximately 3 km distant from each other. Sherman Island is located in the Sacramento–San Joaquin River delta, about 60 km east of San Francisco.

The three ecosystems have Mediterranean-type climates with wet, cool winters and dry, hot summers. In the area of the open grassland and oak/grass savanna, mean annual precipitation is 562 mm, with a standard deviation of 193 mm over the period of 1948–2005. Mean annual air temperature, minimum air temperature in January, and mean maximum air temperature in July are 16.5 °C, 3.5 °C, and 35.4 °C, respectively (using data from the Camp Pardee climate station, ~26 km south of Vaira Ranch). In the area of the peatland pasture, mean annual precipitation is 325 mm, and mean annual air temperature is 15.6 °C (using data from the Antioch climate station, ~10 km south-west of Sherman Island).

The soil of the open grassland is an Exchequer, very rocky silt loam (Lithic Xerorthents), containing 30% sand, 57% silt, and 13% clay, with a bulk density of $1.43 \pm 0.10\ g\ cm^{-3}$ at the surface layer (0–30 cm), a total N content of 0.14%, and a total C content of 1.39%. The soil of the woodland is classified as an Auburn, very rocky silt loam (Lithic Haploxerepts) containing 43% sand, 43% silt, and 13% clay, with a bulk density of $1.61 \pm 0.10\ g\ cm^{-3}$ at the surface layer (0–30 cm), a total N content of 0.11%, and a total C content of 0.95%. The soil of the peatland pasture is classified as a silty loam in the upper 60 cm of the soil profile. It overlays massive peat deposits with thickness >7 m (Drexler et al., 2009). Soil total C in the upper 5 cm is 7.8%; soil total N in the upper 5 cm is 0.57%; bulk density is 1.09–1.32 $g\ cm^{-3}$. Thus, the peatland pasture soil contains total C and N concentrations much higher than the open and understory grassland.

The delta peatland was drained for agriculture 130 years ago. These human activities have caused significant land subsidence via respiration of the most labile peat deposits and compaction due to the presence of cattle. The water table at Sherman Island ranges between 30 and 70 cm below the ground surface and is maintained by a network of ditches and pumping stations. In comparison, the water table is approximately 10 m below the surface at the Tonzi Ranch (Miller et al., 2010)

At the sites of the open and understory grasslands, the current dominant species of annual grasses and forbs include *Brachypodium distachyon*, *Bromus hordeaceous*, *Erodium cicutariu*, *Hypochaeris glabra*, *Trifolium dubium* Sibth., *Trifolium hirtum* All., *Dichelostemma volubile* A., and *Erodium botrys* Cav. These species are invasive and from the Mediterranean Basin (Europe) (Jackson, 1985). At the woodland, blue oak trees (*Quercus douglasii*) dominate the overstory (~194 stems ha^{-1}), and annual grasses occupy the understory and open area. The mean height of the trees is 10.1 m with a standard deviation of 4.7 m. Leaf area index (LAI) of the oak woodland was steady during the growing season at 0.6–0.7. At the peatland pasture site, the ground is covered with patchy, short annual C_3 grass species such as mouse barley (*Hordeum murinum* L.) and pepperweed (*Lepidium latifolium* L.), a broad-leaved perennial herb (Sonnentag et al., 2010). LAI at the peatland pasture ranged from 0.68 to 0.81 in 2009.

2.2. Ecosystem respiration pulses

Flux and meteorological data were measured and processed with the methods described in Xu et al. (2004). A common set of eddy covariance instruments was implemented on a 2-m tripod at the open and understory grassland and on a 3-m tower at the peatland pasture, consisting of a three-dimensional sonic anemometer (Model 1352, Gill Instruments Ltd., Lymington, UK) and an open-path, fast response infrared gas analyzer (IRGA, Li 7500, LI-COR, Inc., Lincoln, Nebraska). The anemometer and the IRGA provide digital output of the fluctuations in three wind components, sonic temperature, water vapor, and CO_2 density. The raw data from each 30-min period were recorded at a rate of 10 Hz and stored on a laptop computer.

We measured air temperature (T_{air}) and relative humidity using a shielded and aspirated sensor (HMP-35 A, Vaisala, Helsinki, Finland), soil temperature (T_s) with thermocouples at 4 cm depth, volumetric soil moisture (θ_v) with a frequency-domain reflectometer probe (ML2x, Delta-T Devices, Burwell, Cambridge, UK), incoming solar radiation with a pyranometer (R_g), incoming photosynthetically active radiation (PAR) with a quantum sensor (Kipp and Zonen PAR-Lite, Delft, Holland), and precipitation (PPT) with a rain gauge (Campbell Scientific Inc., Logan, UT, USA). At the understory grassland site, we calculated understory precipitation by applying an interception coefficient, approximately 0.3, to overstory precipitation measurements; this ratio was derived from the difference in volumetric soil moisture content, θ_v, between open and understory probes measured over a two-day period after rain events. Understory solar radiation was derived from the above-canopy measurement by considering effects of the canopy structure during each hour of the summer months (Ryu et al., 2010). Soil moisture was transformed to soil water potential based on the curve of soil water potential and moisture for the open grassland and understory, respectively (Xu et al., 2004).

Rain-induced respiration pulses were identified by comparing half-hour CO_2 flux measurements with precipitation records (Xu et al., 2004). We then searched for an observable jump in R_{eco}. To quantify the daily-integrated size and shape of an individual respiration pulse, we filled gaps in half-hourly CO_2 flux data using interpolation methods documented in our prior studies (Detto et al., 2010; Ma et al., 2007).

In quantifying the shape, size and duration of the respiration pulses, we defined several metrics relating to the basal R_{eco}, maximum R_{eco} ($MaxR_{eco}$), ending R_{eco}, total cumulative R_{eco} ($\sum R_{eco}$), and pulse duration with daily-integrated R_{eco} values. The basal R_{eco} is the average of R_{eco} over the two or three days preceding the sudden jump in R_{eco}; the ending R_{eco} is the average of R_{eco} over the two or three days at the end of a respiration pulse; $MaxR_{eco}$ is the maximum value of R_{eco} over the entire period of a respiration pulse; the duration of a pulse is defined as the number of days between the date one day before the sudden jump and the date when the value of R_{eco} returns to the basal R_{eco}; $\sum R_{eco}$ is the total amount of CO_2 released over the duration of the pulse.

2.3. Litter-watering experiments

To interpret the rain-induced respiration pulses that we observed in the field with the in situ eddy covariance measurements, we conducted a set of manipulative laboratory and field litter-watering experiments during the summer of 2010. This study involved sampling fresh litter from the field at the start of the senescent period and exposing litter samples to sunlight at the oak/grass savanna site for different durations over the dry summer. We progressively collected subsamples of litter and soil, brought them to the lab, and measured the transient response in respiration rates of combinations of litter, litter and soil, and soil after the addition of water. In the following subsections, we describe the experimental methods and sampling strategies.

2.3.1. Litter cages—treatment in the savanna

Litter cages were made from PVC and aluminum mesh designed to hold senesced plant material while allowing for direct penetration of the full spectrum of incoming radiation as described in (Henry et al., 2008). Litter cages were placed in the field near three randomly selected trees. Plots were established along the four cardinal directions; these plots were 1 m from the tree bole in the shaded treatment and 8 m from the tree bole in the open treatment. Four plots resulted for each radiation treatment for each tree, giving us a total of 12 shaded and 12 open plots in the landscape.

Biomass in the litter cages was collected from 1 m^2 plots of standing dead grass at each established radiation plot following senescence of the understory grass on June 23, 2010. In the lab, the plant litter material was homogenized by gently mixing it, and then dried in a 65 °C oven for about 24 h. After the litter was dried, samples of 2.8–3.2 g were weighed, and the dried senesced material was placed into the litter cages.

Four replicate litter cages were placed in each of the 24 field plots on Day 176 (June 25, 2010), and a replicate cage was harvested from each plot approximately every three weeks, on day 196 (July 15), day 217 (August 5), day 237 (August 28), and day 261 (September 19), all 2010; there was no rainfall during this period that could disturb the samples. On the same dates as the cage harvests, we randomly sampled 36 intact soil cores using a slide hammer and cylindrical core collars 5 cm in diameter and 5 cm in height. To minimize any root effects, we rejected random samples that fell closer than 2 m from tree boles. In the lab, we measured the mass of the litter within each of the harvested litter cages and the field weight of each intact soil core.

2.3.2. Litter-watering treatments

We performed two levels of watering treatments and three levels of litter treatments on the soil cores, resulting in six combined litter-water treatments with six replicates of each. The two water treatments were low (0.5 mm applied over 1 h) and high (2 mm applied over 1 h). These water additions are much smaller than the average precipitation event. The three litter treatments included no litter (none), litter placed in shaded areas (shade), and litter exposed in open canopy areas (open). We also applied the two watering treatments to litter-only samples (excluding the soil core from the treatment) to test whether the water addition increased microbial activity from the litter surface.

From each harvested litter cage, 1.1–1.5 g of litter was weighed and placed above the soil cores by gently placing them within an aluminum foil collar about 2 cm in height fastened to the top of

the soil core. After all the litter-only and soil-litter microcosms were constructed, we incubated them for 48 h at 31 °C, the average summer soil temperature at 2 cm depth at Tonzi Ranch.

After incubation, we measured the basal soil respiration rate for each sample using a LI-820 (Li-Cor Biosciences, Lincoln, NB) in a closed-path non-steady-state flow-through chamber (Livingston and Hutchinson, 1995), with circulation driven by an oil-free diaphragm pump operating at 6 L per min (KNF Nueberger Inc., Trenton, NJ, model N86KNDC). Next, we administered a low distilled water pulse (1.0 mL total, delivered as 0.1 mL every 12 min for an hour) to half the samples and a high distilled water pulse (4 mL total, delivered as 0.4 mL every 12 min for an hour) to the remaining half of the samples in attempts to more closely replicate physical field conditions of rainfall. We measured the CO_2 efflux immediately following the end of water application, then at 1, 2, 4, 8, 16, and 32 h following the watering treatment. The respiration rate of each sample was calculated as a function of the rate of change in CO_2 concentration (Curiel Yuste et al., 2007; Livingston and Hutchinson, 1995).

2.4. Labile C pools involved in respiration pulses

The dynamics of the soil C pools involved in soil CO_2 pulses can be estimated from fitting data with a two-pool, four parameter model (Curiel Yuste et al., 2009; Townsend et al., 1997):

$$C(t) = k_f \times C_f \times e^{-k_f t} + k_s \times C_s \times e^{-k_s t} \quad (1)$$

where $C(t)$, in gC m^{-2} day^{-1}, is the CO_2 flux at the time t; C_f is the C content of the labile C substrates decomposed quickly by soil microbes during the respiration pulse, and C_s is the C content of the recalcitrant C substrates; k_f, in day^{-1}, is the rate constant of the labile C pool, and k_s is the rate constant of the recalcitrant C pool.

This two-pool model is used to estimate the labile and recalcitrant C pools involved in each R_{eco} pulse. The parameters were estimated by fitting a 4-parameter exponential non-linear regression model. This model considers the labile and recalcitrant C pools simultaneously; it provided the most reliable estimation of parameters. We also tried 2- or 3-parameter models that only considered the fast C pool and treated the recalcitrant C pool as a constant, but parameter estimation was not successful, either because the nonlinear regression failed to converge, or because the results were unreasonable.

2.5. Statistical analysis

Statistical analyses were performed by using SAS 9.0 (SAS Institute Inc., Cary, NC, USA). For testing the effects of the litter and water treatments on the respiration rates of samples, we performed the analysis of variance (ANOVA) and the multivariate repeated-measured analysis of variance (MANOVA) with general linear models. Nonlinear regressions were performed for estimating parameters in a variety of empirical curves. We set the significance level to 0.05.

3. Results

3.1. Respiration pulses

Seasonal patterns of R_{eco} followed seasonal distribution of precipitation. R_{eco} remained at a low level during the dry summer (Fig. 1, the open annual grassland, for example), while R_{eco} fluctuated remarkably in other seasons. Sudden jumps of R_{eco} (i.e., respiration pulses) could occur when rain events came in right after the dry summer and could also occur in the spring when rain events came in after a short period of drought. These phenomena repeated year after year.

Respiration pulses varied in shape with different rainfall patterns. Three typical rainfall patterns occurred at our study sites (Fig. 2). When rain events were intensive and clustered within a short period (Fig. 2A), soil moisture increased progressively over three days. R_{eco} spiked and then decayed with time over a 10-day period. In comparison, when rain events were solitary (Fig. 2B), respiration rates were elevated above antecedent rates for a shorter time (about 9 days) because the rain event was too small to fully wet the soil. The third case involved repeated rain events separated by 7–10 days (Fig. 2C). The frequent rain kept the soil moist, and elevated respiration rates were sustained for over 30 days. In these three situations, soil temperature either increased or decreased while soil water potential was decreased gradually, following the wet-up. This indicates that the shapes of the respiration pulses were directly controlled neither by soil temperature nor by soil moisture.

From 2001 to 2010, we identified 26 respiration pulses for the open annual grassland and 26 for the woodland understory. In sum, the two sites had 9 respiration pulses shaped as the first case, 13 as the second case, and 4 as the third case. In addition, 5 pulses were observed at the peatland pasture from 2007 to 2009 (Table 1), including 2 respiration pulses shaped as the first case, 3 as the second case, and 0 as the third case.

On average, the respiration pulses lasted 20 days and ranged between 7 and 46 days (Table 1). At the open grassland site, for example, the shortest respiration pulse lasted 9 days and emitted 5.6 g C m^{-2} of CO_2; it was triggered by a 5.5-mm rain event between days 287 and 296 in 2005. In contrast, the longest respiration pulse lasted 46 days and emitted 137.1 g C m^{-2} of CO_2; it was prompted by 169.4 mm of precipitation between day 285 and 330 in 2010.

Before the respiration pulses were triggered, basal respiration rates (mean ± standard deviation) were 1.33 ± 0.54 g C m^{-2} day^{-1} for the annual grassland, 0.62 ± 0.11 g C m^{-2} day^{-1} for the woodland understory, and 2.58 ± 0.91 g C m^{-2} day^{-1} for the peatland pasture (Table 1). The magnitude of the peak within an individual respiration pulse varied around 4.23 ± 1.41 g C m^{-2} day^{-1} at the annual grassland, 2.26 ± 0.79 g C m^{-2} day^{-1} at in the woodland understory, and 6.19 ± 1.95 g C m^{-2} day^{-1} at the peatland pasture. Similarly, $\sum R_{eco}$ of a single rain-induced respiration pulse was lowest at the woodland understory (24.2 ± 17.8 g C m^{-2}), highest at the peatland pasture (94.6 ± 45.8 g C m^{-2}), and intermediate at the open grassland (44.4 ± 38.0 g C m^{-2}). Overall, the peatland pasture experienced the largest respiration pulses, while the woodland understory experienced the smallest respiration pulses. High standard deviations indicated high variability in the size of the respiration pulses.

3.2. Precipitation effects

Greater precipitation induced greater total amounts of CO_2 emission from a respiration pulse (Fig. 3A). The best fit of the increasing trend was determined by $\Sigma R_{eco} = 131.82(1 - e^{0.0112\,\Sigma PPT})$ with $R^2 = 0.73$ ($p < 0.0001$) for the open annual grassland and $\Sigma R_{eco} = 83.83(1 - e^{0.0222\,\Sigma PPT})$ with $R^2 = 0.84$ ($p < 0.0001$) for the woodland understory. These results indicate that variations in precipitation of rain events explained 73–84% of variations in the total CO_2 productions of respiration pulses at the open grassland and woodland understory sites. During the dry summer, higher temperatures were related to lower R_{eco}. This relationship persisted when rain events occurred (Fig. 3B), suggesting a decoupling between temperature and R_{eco}. In contrast, R_{eco} at the peatland pasture was coupled with temperature increases within the temperature range 10–20 °C (Fig. 3B). The complexity of the peatland pasture site is discussed further in Section 4.

Precipitation amount affected $MaxR_{eco}$ in a non-linear manner, and the open grassland had higher $MaxR_{eco}$ compared to

Table 1
Mean, standard deviation (std), minimum (min), and maximum (max) duration of pulses, basal respiration, ending R_{eco}, maximum daily respiration ($MaxR_{eco}$), total ecosystem respiration (ΣR_{eco}), precipitation (ΣPPT), soil temperature at 4 cm (T_s), and changes in soil water potential near the surface ($\Delta\Psi$) at the open annual grassland, the woodland understory, and the peatland pasture.

Site	Statistics	n	Duration (days)	Basal R_{eco} ($g C m^{-2} day^{-1}$)	$MaxR_{eco}$ ($g C m^{-2} day^{-1}$)	Ending R_{eco} ($g C m^{-2} day^{-1}$)	ΣR_{eco} ($g C m^{-2}$)	ΣPPT (mm)	T_s (°C)	$\Delta\Psi$ (MPa)
Open grassland	Mean	26	20	1.33	4.23	1.37	44.4	36.7	18.7	9.58
	Std	26	10	0.54	1.41	0.40	38.0	47.9	4.5	6.61
	Min	26	9	0.87	0.84	0.74	10.2	0.0	11.5	0.91
	Max	26	46	3.27	7.92	2.04	157.9	169.4	29.1	26.92
Woodland understory	Mean	26	20	0.62	2.26	0.83	24.2	25.8	18.3	8.79
	Std	26	10	0.11	0.79	0.23	17.8	33.2	4.3	7.73
	Min	26	9	0.40	1.29	0.59	5.6	0.0	11.7	1.18
	Max	26	46	0.82	3.97	1.57	85.2	113.9	28.3	33.46
Peatland pasture	Mean	5	24	2.58	6.19	2.65	94.6	28.8	14.1	0.573[a]
	Std	5	7	0.91	1.95	0.26	45.8	28.9	2.8	0.014[a]
	Min	5	12	1.70	3.46	2.31	24.3	8.0	9.6	0.557[a]
	Max	5	31	3.83	8.56	2.92	134.2	79.8	16.5	0.586[a]

[a] Soil volumetric moisture ($cm^3 cm^{-3}$) for the peatland pasture, instead.

the woodland understory (Fig. 4). At the open grassland site, $MaxR_{eco}$ diverged into two groups when precipitation exceeded 20 mm at the open annual grassland and the woodland understory area (Fig. 4), indicating that the same amount of precipitation induced different sizes of respiration pulses at the different sites. The pulses in the top group had higher $MaxR_{eco}$ and usually occurred after a prolonged dry period during the summer, while $MaxR_{eco}$ of the sequential pulses were lower and usually followed the former pulses. Difference in $MaxR_{eco}$ between the two groups was ~2 $g C m^{-2} day^{-1}$ in the open grassland, while difference was <1 $g C m^{-2} day^{-1}$ in the woodland understory, given the same amount of precipitation. $MaxR_{eco}$ at the understory site

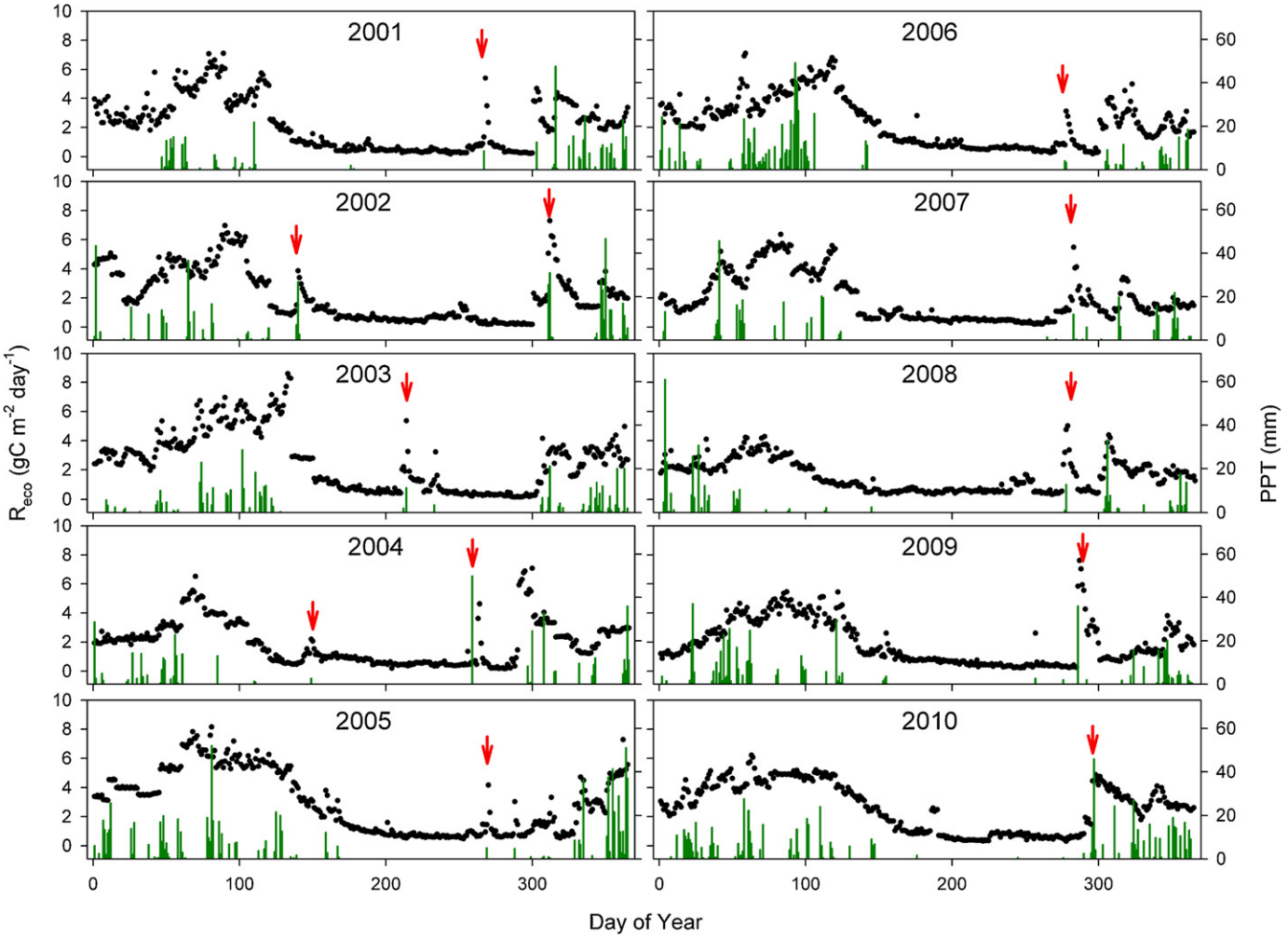

Fig. 1. Comparing daily-integrated ecosystem respiration (R_{eco}) and precipitation (PPT) at Vaira Ranch from 2001 to 2010: respiration pulses triggered by isolated rain events are identified for those occurring in late spring or early autumn, examples shown by arrows.

Table 2
ANOVA results for testing overall effects of harvesting date of litter samples, watering, and litter cover on the total amount of CO_2 flux ($\sum R$) and the maximum CO_2 flux (R_{max}) during the measuring period.

Dependent variable	Source	DF	Mean square	F	$P > F$	R^2
$\sum R$	Harvesting date	2	119.937	93.97	<0.0001	0.73
	Watering	1	61.845	48.46	<0.0001	
	Litter	2	22.458	17.6	<0.0001	
R_{max}	Harvesting date	3	267.880	39.29	<.0001	0.5
	Watering	1	34.009	4.99	0.0272	
	Litter	2	45.470	6.67	0.0017	

was about 70% of that at the open grassland. This difference was the same as the difference in precipitation once the understory precipitation was corrected for canopy interception. However, when we compared $MaxR_{eco}$ of the top group pulses between the open grassland and the woodland understory, $MaxR_{eco}$ at the understory site was ~60% of that at the open grassland site. This outcome suggests that $MaxR_{eco}$ at the open grassland may be enhanced in comparison to the understory.

Precipitation effects were associated with changes in soil water potential ($\Delta\Psi$, i.e., differences between the maximum Ψ and the initial Ψ during the period of a respiration pulse) because microbes respond to changes in water potential, not changes in volumetric water content. $\Delta\Psi$ was positively correlated to precipitation for the two sites ($F = 21.47$; $p < 0.0001$). Fig. 5 shows an example of a rain-induced respiration pulse in 2010. In this case, 168 mm of precipitation deposited on the grassland and 114 mm

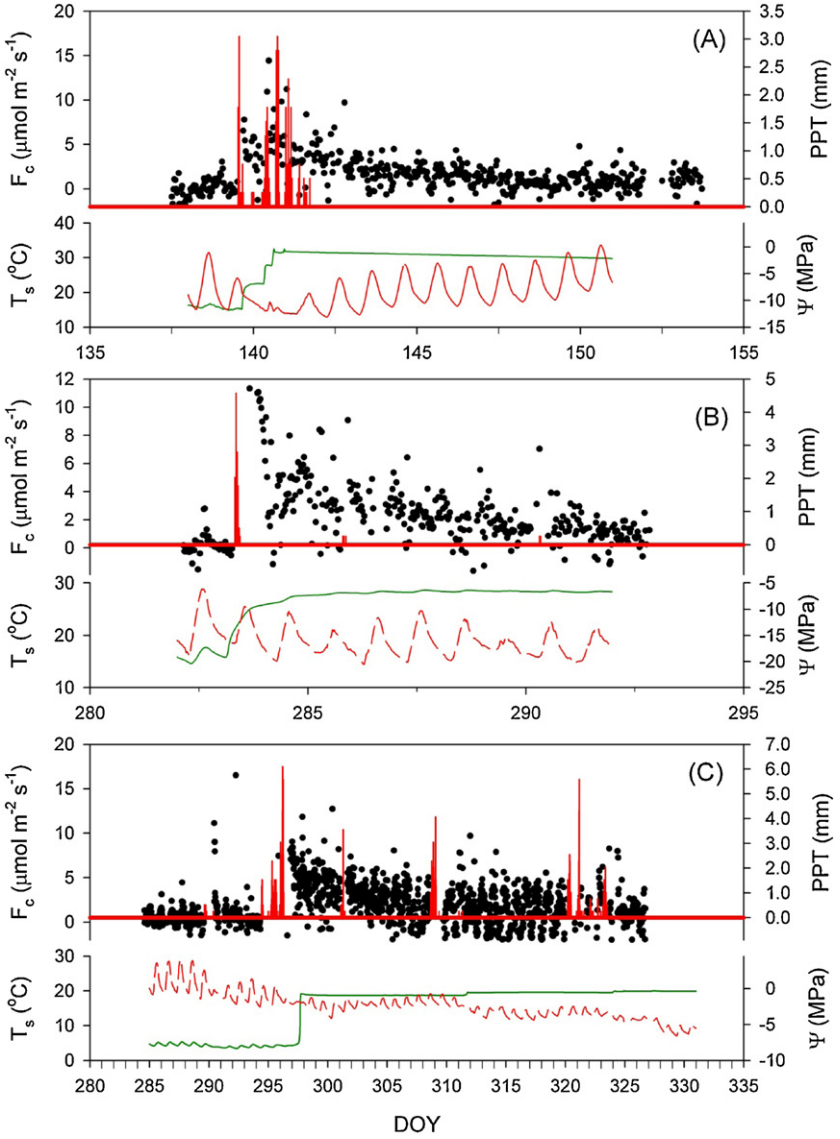

Fig. 2. Examples of respiration pulses at the open annual grassland, presented with half-hourly CO_2 flux (F_c, in dots), precipitation (PPT, in bars), soil surface moisture (Ψ, in lines), and soil temperature at 4 cm (T_s, in dashed lines): (A) in the late spring of 2002; (B) in the late summer of 2004; (C) in the early autumn of 2010.

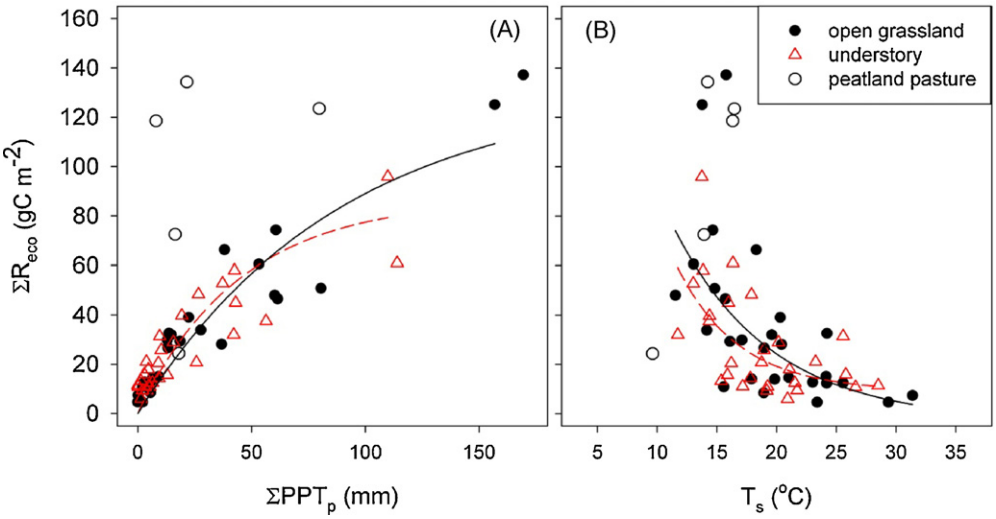

Fig. 3. The total amount of ecosystem respiration (ΣR_{eco}) in response to the total precipitation of the pulse (ΣPPT) and soil temperature (T_s) over the course of respiration pulses at the open annual grassland, the woodland understory, and the peatland pasture. Solid curves are regression fittings for the open annual grassland; dashed curves are for the woodland understory.

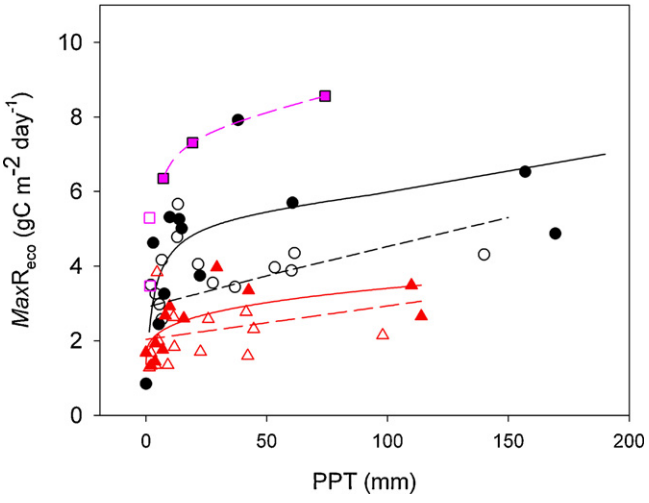

Fig. 4. Maximum of daily ecosystem respiration ($MaxR_{eco}$) in response to precipitation right before rain pulses (PPT) at the open annual grassland (in solid or open circles), the woodland understory (in solid or open triangles), and the peatland pasture (in solid or open squares). Solid symbols represent pulses immediately after a long dry period; open symbols represent sequential pulses. Solid and dashed lines are regression fittings for each group of data.

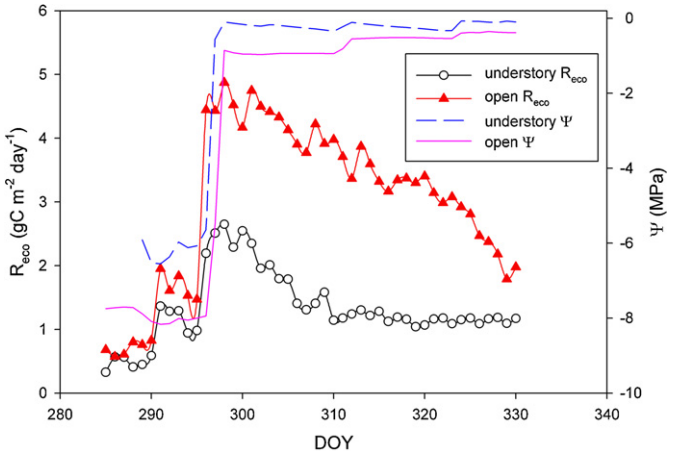

Fig. 5. Comparison of a pair of respiration pulses that occurred at the open grassland and the understory site between days 285 and 330 in 2010, coupled with changes in soil water potential (Ψ).

of rainfall was received by the understory grass. This amount of rainfall caused mean soil water potential to decrease by 8 MPa at the grassland and by 6 MPa at the understory. Consequently, daily integrated R_{eco} increased from 0.67 to 4.87 g C m^{-2} day^{-1} at the open grassland and from 0.32 to 2.65 g C m^{-2} day^{-1} at the understory.

It seems reasonable that differences in precipitation controlled CO_2 efflux from the woodland understory area and the open grassland. Grass under the oak woodland received 33% less precipitation than the open grassland because the woodland intercepted this precipitation. In turn, we observed that the grass understory produced 54% of the CO_2 emitted from the open grassland (Fig. 4). If the CO_2 fluxes of the respiration pulse were entirely due to the increase in $\Delta\Psi$, the change in the magnitude of the CO_2 fluxes would remain closer to the relative fraction of precipitation at the two sites. Among the 26 pairs of respiration pulses, eight pairs had fraction of $MaxR_{eco}$ close to the relative fraction of precipitation that was either received by the open grassland or fell through the oak woodland overstory, including the two pulses that occurred in the early dry season; these early season pulses were stimulated by small rain events (precipitation <50 mm). With intense rain events, the differential fraction of CO_2 fluxes at the two was smaller than the differential fraction of precipitation received by them because the canopy becomes saturated with moisture. Other than precipitation or change in soil water potential, what else might be responsible for the inter-site differences between the grassland and understory? To answer this question, we studied the possible effects of litter, especially for litter exposed in the field during the dry season, on the peak values of respiration pulses.

3.3. Litter effects

In the litter-watering experiment, the CO_2 efflux increased rapidly within two hours for all replicates that contained soil and then decreased gradually over the course of 16–32 h, similar to the respiration pulses observed in the field (Fig. 6). Such pulse-like changes in CO_2 efflux were statistically significant ($F = 29.99$, $p < 0.0001$). The total amount of CO_2 efflux for each pulse differed significantly ($F = 8.25$, $p = 0.0047$) between the low- and high-level watering treatments (Table 2). Mean CO_2 efflux was 1.05 ± 0.09 μmol m^{-2} s^{-1} for the low level of watering, which was lower than the CO_2 efflux from the samples with the high level

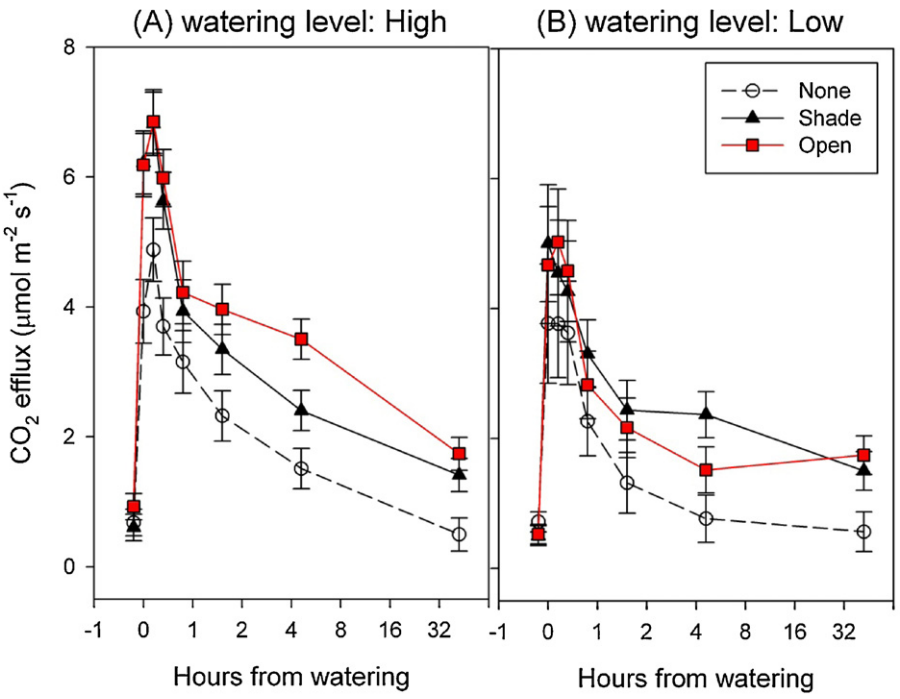

Fig. 6. Pulse-shaped CO_2 efflux from soil samples without litter covering (none) and from soil samples covered with litter treated under sunlight in the open (open) or shaded (shade) area, with two levels of watering experiment. Bars are standard errors.

of watering (1.41 ± 0.09 μmol m^{-2} s^{-1}). We also measured the CO_2 efflux from the litter-only samples (0.01 ± 0.11 μmol m^{-2} s^{-1}), which was not significantly different from zero. This outcome indicates that the large CO_2 efflux following watering came entirely from the soil cores.

For soil samples, the total amount of CO_2 flux ($\sum R$) and the maximum CO_2 flux (R_{max}) both differed significantly across the three levels of litter treatment at the high level of watering ($F = 5.40$, $p = 0.0066$ for $\sum R$; $F = 7.86$, $p = 0.0008$ for R_{max}) but not at the low level of watering. Overall, the CO_2 efflux produced from soil samples with litter differed significantly from soil samples without litter although the results were quite similar between litter from the open area and litter from the shaded area (Fig. 7).

Litter harvested on different dates produced significant differences in the CO_2 efflux pulses (MANOVA test: $F = 28.10$, $p < 0.0001$). Interestingly, the greatest significant difference occurred during the middle of the summer, instead of at the end of summer. We examined meteorological variables including solar radiation, air temperature, soil moisture, and wind speed during the dry period when the litter-watering treatments were applied. All meteorological variables were stable, decreasing slightly in the season. Daily integrated solar radiation was 15.2–16.9 MJ m^{-2} day^{-1}; daily mean air temperature was 22.6–23 °C; daily mean soil moisture was 8%–9%; soil water potential was −3.1 to −2.3 MPa; daily mean wind speed was 0.53–0.55 m s^{-1}. These variables were quite homogenous over such hot, dry summer days.

Tower-derived respiration data showed a significant relationship between $MaxR_{eco}$ and solar radiation during the previous dry season (Q_{dry}) for respiration pulses enhanced by litter (Fig. 8). In general, $MaxR_{eco}$ were positively related to the incident solar radiation during the previous dry period. Notice that $MaxR_{eco}$ was normalized by precipitation to minimize effects of precip-

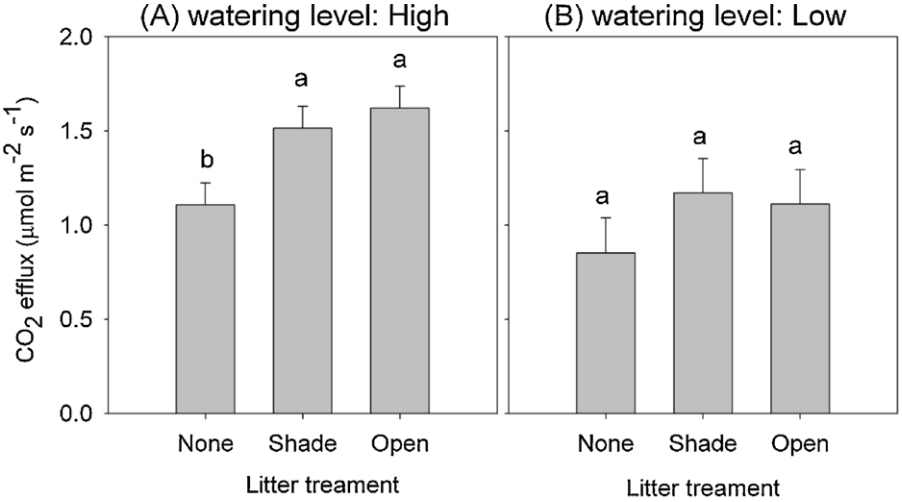

Fig. 7. Comparisons of CO_2 pulses from soil samples without litter covering (none) and from soil samples covered with litter treated under sunlight in the open (open) or shaded (shade) area, with two levels of watering experiment. Bars are standard errors.

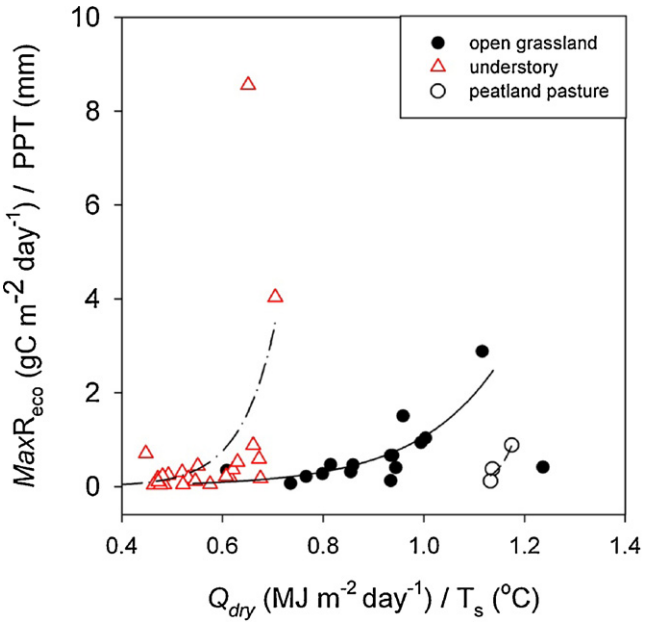

Fig. 8. Maximum values of ecosystem respiration ($MaxR_{eco}$) per millimeter of precipitation (PPT) during each pulse period versus incident solar radiation (Q_{dry}) per degree Celsius (T_s) during antecedent dry season at the open annual grassland (solid), the woodland understory (dash-dot), and the peatland pasture (dash).

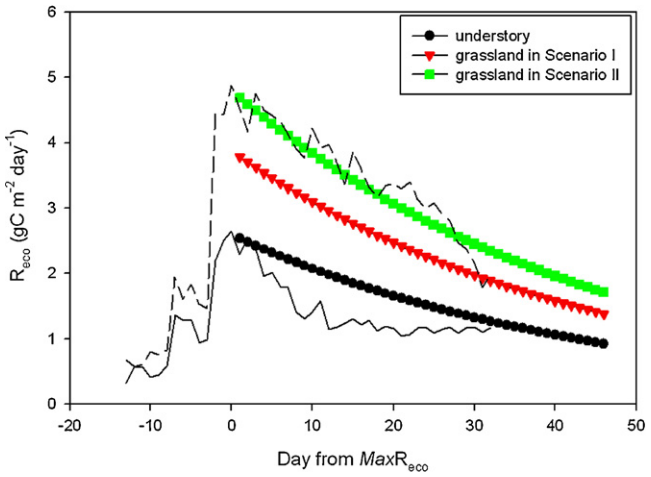

Fig. 9. Model results of the decay trend of respiration pulses in Scenario I and Scenario II (see text), compared with field data from the open grassland (dashed line) and the understory site (solid line) between Days 285 and 330 in 2010.

itation, and that Q_{dry} was normalized by T_s to reduce effects of temperature during the dry period. The open grassland had higher solar radiation levels than the shaded woodland understory. Best fits of the non-linear trend are $MaxR_{eco}/PPT = e^{3.318(Q_{dry}/T_s - 1.021)}$ ($R^2 = 0.27$, $p = 0.0076$) for the open annual grassland and $MaxR_{eco}/PPT = e^{14.54(Q_{dry}/T_s - 0.619)}$ ($R^2 = 0.24$, $p = 0.0119$) for the woodland understory. Such a trend was not statistically significant at the peatland pasture: $MaxR_{eco}/PPT = e^{31.153(Q_{dry}/T_s - 1.79)}$ ($R^2 = 0.91$, $p = 0.1939$).

3.4. Labile C pools involved in respiration pulses

C_f estimated with the 4-parameter exponential decay model (Eq. (1)) varied from pulse to pulse. The mean and standard error of C_f were 45.0 ± 10.2, 22.3 ± 11.3, and 156.8 ± 26.1 g C m^{-2} at the open annual grassland, the woodland understory, and the peatland pasture, respectively. These estimates of C_f differed significantly across sites ($F = 11.18$, $p = 0.0001$). C_f was greatest at the peatland pasture. The results of ANOVA supported the finding that k_f across the three sites did not differ significantly ($F = 1.54$, $p = 0.2256$). That is, the size of a respiration pulse was determined primarily by the value of C_f. Thus, we could compare paired respiration pulses simultaneously occurring at the open grassland and the woodland understory area.

In further modeling, we first restructured the decay trend of the respiration pulse for the open grassland with the parameters estimated from field data. Then we used the same set of parameters for modeling the decay trend of the understory pulse and the open grassland in two scenarios. The first scenario occurred when the fraction of CO_2 fluxes between the woodland understory and the open grassland was similar to the fraction of precipitation between the two sites. In contrast, the fraction of CO_2 fluxes was lower than the fraction of precipitations between the two sites in the second scenario. Modeling showed that the size of the respiration pulse from the open grassland was larger than that from the understory, but the CO_2 released from the open grassland in Scenario II was approximately 24% higher than that in Scenario I (Fig. 9). This modeling result concurs with the information displayed in Figure 4.

4. Discussion

This study focuses on rain-induced respiration pulses that mainly occur at the end of the dry season when heterotrophic respiration dominates R_{eco} in the ecosystem. These respiration pulses depend directly upon microbial activities, and they are distinctive from the pulses that occur in the wet season. In the wet season, frequent rainfall events keep the soil moist. Plant autotrophic respiration (i.e., aboveground parts and roots) contributes a significant fraction of ecosystem respiration because recent photosynthetic products affect soil C pools at the ecosystem level, and these processes interact with changes in microbial community composition (Vanderbilt et al., 2008). In contrast, when vegetation is dead or dormant due to drought, labile C substrates from recent plant photosynthesis are reduced and much less C substrate is transported to the roots and microbes (Moorhead and Sinsabaugh, 2006). Consequently, heterotrophic respiration dominates the signal of R_{eco}.

The occurrence of respiration pulses is a result of emerging processes of many abiotic and biotic factors. First, precipitation rewets dry soils directly and causes significant changes in soil water potential (Fierer and Schimel, 2003; Unger et al., 2010; Xu et al., 2004). Second, soil microbial activity stimulated by this change in soil water potential immediately results in jumps in CO_2 efflux (Huxman et al., 2004; Lee et al., 2004; Xu et al., 2004). Third, CO_2 efflux must decrease after the first jump because of decreases in the availability of labile C substrates (Curiel Yuste et al., 2009; Kuzyakov et al., 2000).

Differences between ending R_{eco} and basal R_{eco} suggest that additional processes emerge. In some cases, at the end of a pulse, the value of R_{eco} returns to original basal R_{eco} at the starting point, meaning that the majority of labile C substrates available must be triggered by precipitation. In other cases, ending R_{eco} is greater than basal R_{eco} This may indicate additional labile C substrates decomposed by soil microbes (Kuzyakov, 2010; Kuzyakov et al., 2000). In the field, outcomes can differ when respiration pulses are constantly stimulated by multiple rain events. During a long period of rain, a respiration pulse could last much longer. Toward the end of this type of respiration pulse, the net ecosystem exchange of CO_2 during the daytime becomes negative, indicating that photosynthesis kicks in. At this moment, labile C substrates triggered by precipitation diminish but are still available to soil microbes. Meanwhile, sufficient soil moisture and more labile C substrates of soil organic matter support increases in root and soil microbial

activities. As a result, the ending R_{eco} could be much greater than the basal R_{eco}.

The difference in basal R_{eco} across sites is probably due to site-specific conditions such as soil C content and presence of vegetation. The open and understory annual grasslands both have very low basal R_{eco} once grasses die out. In contrast, the peatland pasture has higher basal R_{eco}. One direct reason is because the peatland has higher soil C content. Although vegetation is alive at the peatland pasture because it is perched above a shallow water table, soil microbes respond to changes in water conditions much faster than plants do during the specific period of respiration pulses (Kuzyakov, 2010).

The size of rain-induced respiration pulses depends directly on the timing and amount of triggering precipitation, similar to the results of previous studies (Xu et al., 2004). However, a key aspect of precipitation effects is sudden changes in soil water potential. This study also investigated effects of temporal patterns of precipitation on soil moisture over the period of respiration pulses. In the field, soil moisture could increase either sharply or gradually. When precipitation is less intense, the soil rewetting process is slower, resulting in slower changes in soil water potential. Consequently, soil microbes may release smaller amounts of cytoplasmic solutes, and soil organic carbon protected in soil microaggregates may be released more slowly and may be smaller in magnitude (Fierer and Schimel, 2003; Kuzyakov et al., 2000; Unger et al., 2010). As a result, the size of respiration pulses is smaller because the availability of the fast organic sources for soil microbes is limited, as suggested in soil incubation studies (Curiel Yuste et al., 2007). In contrast, larger or more intense rain events generate respiration pulses with a faster rise and longer duration. Such respiration pulses cause more CO_2 to be released from the soil to the atmosphere.

Whether a rain event can induce a respiration pulse depends on how dry the soil is (Huxman et al., 2004; Xu et al., 2004). In this study, we investigated respiration pulses not only occurring at the end of the dry summer but also in two cases in the late spring, shortly after the grass died in the open grassland and the woodland understory. The sizes of these two pulses followed the relationship drawn from the late-summer pulses without litter effects. Litter effects are not applicable to the late-spring cases because litter has not had enough time to undergo intensive photodegradation. Alternately, litter effects are testable with the late-summer pulses. Our modeling results of Scenarios I and II match our field observations.

Together with precipitation, litter played an important role in determining the size of the respiration pulse. In the litter-watering experiments, the treatments with litter on top of the soil resulted in more CO_2 efflux. When water enters dry soils, the rewetting process starts from the top of the surface litter layer. Rainfall leaches soluble C compounds from surface litter to the soil (Kuzyakov et al., 2000), and soluble C substrates can be favorable to a group of decomposers, called "opportunist microorganisms" in a theoretical litter-microbial interaction model (Moorhead and Sinsabaugh, 2006). When similar processes occur in the field, litter effects can amplify the difference in respiration pulse between the woodland understory and the open grassland, beyond the effects of canopy interception.

The reason that litter can provide soluble C substrates to the soil with rain events is that abiotic degradation occurs in dry conditions when bio-degradation is inhibited by lack of water. Under harsh dry conditions, litter continuously loses mass (Henry et al., 2008; Montana et al., 1988; Moorhead and Callaghan, 1994; Moorhead and Reynolds, 1989), and CO_2 flux is measureable (Huxman et al., 2004; Inglima et al., 2009; Xu et al., 2004). A growing body of literature provides evidence that these phenomena result from photodegradation (Kuzyakov, 2010; Moorhead and Callaghan, 1994; Rutledge et al., 2010). Our data support this assertion with the fact that solar radiation during the dry period is related to the size of respiration pulses. Unfortunately, the litter-watering experiments did not show statistically significant differences between shade and open treatment of litters, likely due to the relatively small rates of watering that were prescribed. The intensity of precipitation could reach 10–38 mm h^{-1} at the open grassland. Thus, for future studies, the litter-watering experiments should use greater levels of watering, which will wash more labile carbon from the litter to the soil. It is also necessary to consider choosing larger soil cores, both in diameter and in depth, to manipulate higher levels of watering treatment. Certainly, many other abiotic processes, like thermal effects, wind fragmentation, and animal activities (Austin and Ballare, 2010) may also affect litter decomposition in dry, hot conditions.

The peatland pasture is a contrasting case. It was grazed all year round. We suspect extra labile C substrates were supplied to soil microbes at the peatland pasture because of excrement deposition and carbon exudates from plant roots. Quantifying effects of these various processes can be difficult but interesting.

In this study, we estimated the labile C pool involved in respiration pulses by fitting the 4-parameter exponential model. The amount of recalcitrant C substrates was much smaller than C_f ($C_s \ll C_f$) at our study sites, as was the rate constant of the recalcitrant C pool ($k_s \ll k_f$). Thus, soil microbes use up labile C pool much faster than recalcitrant soil C pools during respiration pulses. Our results showed high variability in C_f. Compared to the values of C_f from a previous study (Curiel Yuste et al., 2009), the labile C pool involved in respiration pulses in the field is much greater than that in the soil incubation samples. One reason for this outcome is the limited size of soil cores. The other reason is litter effects. At our study sites, photo-degraded litter may have enhanced the size of respiration pulses more than 20%. This result supports the hypothesis that more labile C input from the degraded litter layer could stimulate larger respiration pulses. In field conditions, we are essentially losing labile C from the soil, straw, or the fraction of straw that becomes wet and in contact with the soil. These C pools differ in size and play different yet complementary roles in fueling rain-induced respiration pulses with variable sources of labile C substrates. However, we still know little about how these C pools interact with one another. For future ecosystem-level studies, quantifying the effects of rain-induced respiration pulses on relatively recalcitrant soil C pools may be important.

5. Conclusion

In this study, we analyzed a decade-long dataset of rain-induced respiration pulses observed at the ecosystem level. These data were explored based on coincident environmental conditions, a litter-watering experiment, and modeling calculations. New insights associated with the occurrence and size of rain-induced respiration pulses emerged. First, the occurrence of rain-induced respiration pulses depends primarily on the dryness of the soil. As long as the soil experiences significant drought, respiration pulses will be induced by rain events. Thus, respiration pulses may occur at any time of the dry season of a semi-arid or arid ecosystem, and respiration pulses may occur in other types of ecosystems following serious drought events. Second, precipitation is the main factor that determines the size of respiration pulses, but effects of litter with antecedent photodegradation are considerable if the triggering precipitation is large enough. Third, biotic and abiotic processes involved in respiration pulses are variable from pulse to pulse. Besides the direct effects of precipitation, which causes soil rewetting and stimulates soil microbes to consume labile C substrates, photo-degraded litter could contribute a significant amount of labile C substrates to the soil and consequently enhance the size of respiration pulses. These findings may help to incorporate

features of respiration pulses into models of terrestrial carbon balance.

Acknowledgements

This research was conducted at a site that is a member of the AmeriFlux and FLUXNET networks, and this research was supported in part by the Office of Science (BER), the U.S. Department of Energy (DE-FG02-03ER63638), and the Western Regional Center of the National Institute for Global Environmental Change under Cooperative Agreement (DE-FC02-03ER63613). This study is also partially supported by the National Science Foundation (DEB-0317139), the Kearney Soil Science Foundation, and the California Agricultural Experiment Station. We gratefully thank Mr. Ted Hehn for his technical support. Thank you to Mr. Joe Verfaillie for his technical and editorial helps. Thank you to Dr. Laurie Koteen for her comments and editorial help. We appreciate Mr. Russell Tonzi and Mr. Fran Vaira for allowing us to access their ranch for scientific research.

References

Austin, A.T., Ballare, C.L., 2010. Dual role of lignin in plant litter decomposition in terrestrial ecosystems. Proceedings of the National Academy of Sciences of the United States of America 107 (10), 4618–4622.

Austin, A.T., Vivanco, L., 2006. Plant litter decomposition in a semi-arid ecosystem controlled by photodegradation. Nature 442 (7102), 555–558.

Baldocchi, D.D., Tang, J., Xu, L., 2006. How switches and lags in biophysical regulators affect spatio-temporal variation of soil respiration in an oak-grass savanna. Journal Geophysical Research, Biogeosciences 111, G02008, doi:10.1029/2005JG000063.

Baldocchi, D.D., Xu, L.K., Kiang, N., 2004. How plant functional-type, weather, seasonal drought, and soil physical properties alter water and energy fluxes of an oak-grass savanna and an annual grassland. Agricultural and Forest Meteorology 123 (1-2), 13–39.

Birch, H.F., 1958. Pattern of humus decomposition in East African soils. Nature 181 (4611), 788–788.

Brandt, L.A., Bohnet, C., King, J.Y., 2009. Photochemically induced carbon dioxide production as a mechanism for carbon loss from plant litter in arid ecosystems. Journal of Geophysical Research-Biogeosciences 114, G02004, doi:10.1029/2008JG000772.

Curiel Yuste, J., et al., 2007. Microbial soil respiration and its dependency on carbon inputs, soil temperature and moisture. Global Change Biology 13 (9), 2018–2035.

Curiel Yuste, J., Ma, S., Baldocchi, D.D., 2009. Plant–soil interactions and acclimation to temperature of microbial-mediated soil organic matter decomposition may affect predictions of soil CO_2 efflux. Biogeochemistry 98, 127–138.

Detto, M., Baldocchi, D.D., Katul, G.G., 2010. Scaling properties of biologically active scalar concentration fluctuations in the surface layer over a managed peatland. Boundary Layer Meteorology, doi:10.1007/s10546-010-9514-z.

Drexler, J.Z., de Fontaine, C.S., Brown, T.A., 2009. Peat accretion histories during the past 6,000 years in the marshes of the Sacramento-San Joaquin Delta CA USA. Estuaries and Coasts 32, 871–892.

Fierer, N., Schimel, J.P., 2002. Effects of drying-rewetting frequency on soil carbon and nitrogen transformations. Soil Biology & Biochemistry 34 (6), 777–787.

Fierer, N., Schimel, J.P., 2003. A proposed mechanism for the pulse in carbon dioxide production commonly observed following the rapid rewetting of a dry soil. Soil Science Society of America Journal 67 (3), 798–805.

Henry, H.A.L., Brizgys, K., Field, C.B., 2008. Litter decomposition in a California annual grassland: interactions between photodegradation and litter layer thickness. Ecosystems 11 (4), 545–554.

Huxman, T.E., et al., 2004. Precipitation pulses and carbon fluxes in semiarid and arid ecosystems. Oecologia 141, 254–268.

Inglima, I., et al., 2009. Precipitation pulses enhance respiration of Mediterranean ecosystems: the balance between organic and inorganic components of increased soil CO_2 efflux. Global Change Biology 15 (5), 1289–1301.

Jackson, L.E., 1985. Ecological origins of California's Mediterranean grasses. Journal of Biogeography 12 (4), 349–361.

Jarvis, P., et al., 2007. Drying and wetting of Mediterranean soils stimulates decomposition and carbon dioxide emission: the Birch effect. Tree Physiology 27 (7), 929–940.

Kuzyakov, Y., 2006. Sources of CO_2 efflux from soil and review of partitioning methods. Soil Biology and Biochemistry 38 (3), 425–448.

Kuzyakov, Y., 2010. Priming effects: interactions between living and dead organic matter. Soil Science Society of American Journal 42, 1363–1371.

Kuzyakov, Y., Friedel, J.K., Stahr, K., 2000. Review of mechanisms and quantification of priming effects. Soil Biology & Biochemistry 32, 1485–1498.

Lee, X., Wu, H.-J., Sigler, J., Oishi, C., Siccama, T., 2004. Rapid and transient response of soil respiration to rain. Global Change Biol 10 (6), 1017–1026.

Livingston, G.P., Hutchinson, R.L., 1995. Enclosure-based measurement of trace gas exchange: applications and sources of error. In: Matson, P.A., Harriss, R.C. (Eds.), Biogenic Trace Gases: Measuring Emissions from Soil and Water. Blackwell Scientific Publications, Oxford, pp. 14–51.

Ma, S.Y., Baldocchi, D.D., Xu, L.K., Hehn, T., 2007. Inter-annual variability in carbon dioxide exchange of an oak/grass savanna and open grassland in California. Agricultural and Forest Meteorology 147 (3-4), 157–171.

Miller, G., Chen, X., Rubin, Y., Ma, S., Baldocchi, D., 2010. Groundwater uptake by woody vegetation in a semi-arid oak savanna. Water Resources Research 46, W10503, doi:10.1029/2009WR008902.

Montana, C., Ezcurra, E., Carrillo, A., Delhoume, J.P., 1988. The decomposition of litter in grasslands of northern Mexico: a comparison between arid and non-arid environments. Joural of Arid Environment 14, 55–60.

Moorhead, D.L., Callaghan, T., 1994. Effects of increasing ultraviolet B radiation on decomposition and soil organic matter dynamics: a synthesis and modelling study. Biology and Fertility of Soils 18 (1), 19–26.

Moorhead, D.L., Reynolds, J.F., 1989. Mechanisms of surface litter mass loss in the northern Chihuahuan desert: a reinterpretation. Journal of Arid Environments 16 (2), 157–163.

Moorhead, D.L., Sinsabaugh, R.L., 2006. A theoretical model of litter decay and microbial interaction. Ecological Monographs 76 (2), 151–174.

Qi, Y., Xu, M., 2001. Separating the effects of moisture and temperature on soil CO_2 efflux in a coniferous forest in the Sierra Nevada Mountains. Plant and Soil 237, 15–23.

Reichstein, M., et al., 2002. Ecosystem respiration in two Mediterranean evergreen Holm Oak forests: drought effects and decomposition dynamics. Functional Ecology 16 (1), 27–39.

Rutledge, S., Campbell, D.I., Baldocchi, D., Schipper, L.A., 2010. Photodegradation leads to increased carbon dioxide losses from terrestrial organic matter. Global Change Biology 16 (11), 3065–3074.

Ryu, Y., et al., 2010. How to quantify tree leaf area index in an open savanna ecosystem: a multi-instrument and multi-model approach. Agricultural and Forest Meteorology 150 (1), 63–76.

Sonnentag, O., et al., 2010. Carbon dioxide exchange of a pepperweed (*Lepidium latifolium* L.) infestation: how do flowering and mowing affect canopy photosynthesis and autotrophic respiration? Journal of Geophysical Research, doi:10.1029/2010JG001522.

Townsend, A.R., Vitousek, P.M., Desmarais, D.J., Tharpe, A., 1997. Soil carbon pool structure and temperature sensitivity inferred using CO_2 and $^{13}CO_2$ incubation fluxes from five Hawaiian soils. Biogeochemistry 38 (1), 1–17.

Unger, S., Maguas, C., Pereira, J.S., David, T.S., Werner, C., 2010. The influence of precipitation pulses on soil respiration – Assessing the Birch effect by stable carbon isotopes. Soil Biology & Biochemistry 42 (10), 1800–1810.

Vanderbilt, K.L., White, C.S., Hopkins, O., Craig, J.A., 2008. Aboveground decomposition in arid environments: results of a long-term study in central New Mexico. Journal of Arid Environments 72 (5), 696–709.

Xu, L., Baldocchi, D.D., 2004. Seasonal variation in carbon dioxide exchange over a Mediterranean annual grassland in California. Agricultural and Forest Meteorology 123 (1–2), 79–96.

Xu, L.K., Baldocchi, D.D., Tang, J.W., 2004. How soil moisture, rain pulses, and growth alter the response of ecosystem respiration to temperature. Global Biogeochemical Cycles 18 (4).